Chinese Journal of Structural Chemistry 42 (2023) 100032

Contents lists available at ScienceDirect

Chinese Journal of Structural Chemistry

journal homepage: www.journals.elsevier.com/chinese-journal-of-structural-chemistry

Review

Exploring the structural properties of cathode and anode materials in Li-ion battery via neutron diffraction technique

Yuxi Luo [1], Xiaoyu Gao [1], Mingjie Dong [1], Tao Zeng [1], Ziwei Chen, Maolin Yang, Zhongyuan Huang, Rui Wang, Feng Pan [**], Yinguo Xiao [*]

School of Advanced Materials, Peking University, Shenzhen Graduate School, Shenzhen, 518055, China

ARTICLE INFO

Keywords:
Neutron diffraction
Lithium-ion battery
Cathode and anode materials
In operando characterization

ABSTRACT

As a unique microprobe for structure and dynamics of materials, neutron possesses superior ability in penetration as well as sensitivity for light and magnetic elements in comparison with X-ray and electron. As for the research and development of lithium-ion batteries (LIBs), neutron diffraction techniques play an indispensable role in exploring the structural properties of various electrode materials, especially the detailed structural evolution of cathode and anode materials during electrochemical cycling. Moreover, based on thorough analysis of neutron diffraction results, an in-depth and systematic understanding of some fundamental mechanisms, such as the formation mechanism of defects and migration mechanism of lithium ions, could also be established, which is essential for the development of high-performance electrode materials for the next-generation LIBs. Nevertheless, that technique would not seem to be widely applied yet in comparison with the application of X-ray diffraction and more attention should be paid. To demonstrate the advantages of neutron diffraction technique in research of LIBs materials, this work systematically summarizes representative neutron diffraction studies on exploring structural details hidden in electrode materials and on probing structural evolution of electrode materials during charge/discharge processes. Prospects for further applications of neutron diffraction techniques in research of LIBs are also put forward.

1. Introduction

It is well known that clean energy sources such as tidal energy, hydrogen energy, biological energy and nuclear energy can alleviate the shortage of stocks and environmental pollution caused by the rapid consumption of fossil energy. However, due to the intermittency and variability of renewable energy sources, it is extremely difficult to integrate electricity generated from renewable energy sources into a power grid with complex loads. Therefore, to develop energy storage technology is of great significance because it can be considered as one of the best solutions matched well with the output characteristics of various renewable energy sources. As one of the most important energy storage technologies, battery energy storage system plays a pivotal role in meeting electricity demands since it can store electricity and then release electricity according to the customers' requirement. Among the various kinds of batteries, LIBs show obvious advantages due to their outstanding electrochemical performance, good cycling performance and no memory effect [1], which are used in the field of power energy.

Research on LIBs can be traced back to the early 1900s. In 1913, the Professor Gilbert N. Lewis published a paper for the first time to study the electrochemical potential of lithium metal as the negative electrode of lithium batteries [2]. It was not until around the 1970s that Panasonic of Japan and NASA developed the first commercial primary lithium battery based on lithium metal based on previous research. In 1973, Stanley Whittingham of Exus Oil Company realized electrochemical reversible intercalation and removal of lithium ions based on TiS_2 material with layered structure and developed the first lithium metal secondary battery [3]. In 1985, William S. Harris from the University of California applied organic circular carbonate as electrolyte in lithium metal batteries, which opened up the beginning of organic electrolyte. It greatly promoted the commercialization process of lithium-ion batteries. In 1988, Murray Company of Canada launched the first commercial lithium secondary battery based on lithium metal and MoS_2 material, marking the maturity of lithium metal secondary battery [4].

The new generation of rechargeable LIBs mainly relies on the lithium ion intercalation and deintercalation between the positive and the

---

[*] Corresponding author.

[**] Corresponding author.

E-mail addresses: panfeng@pkusz.edu.cn (F. Pan), y.xiao@pku.edu.cn (Y. Xiao).

[1] Yuxi Luo, Xiaoyu Gao, Mingjie Dong and Tao Zeng contribute equally to this work.

https://doi.org/10.1016/j.cjsc.2023.100032
Received 8 December 2022; Received in revised form 6 February 2023; Accepted 9 February 2023

negative electrodes to achieve the charging and discharging function. Typical cathode materials include $LiCoO_2$, $LiNiO_2$ and $LiMnO_2$, among which $LiCoO_2$ can be traced back to the 1970s [5]. All these three materials possess layered structure in common but have respective drawbacks with respect to electrochemical performances. Therefore, in the mid-1990s, people started to integrate nickel, cobalt and manganese into transition metal (TM) layers [6,7], and fabricate ternary cathode materials. After continuous exploration and summary, the layered oxides $LiNi_xMn_yCo_zO_2$ (NMC, $x + y + z = 1$) have been well developed and achieved great commercial success [8,9]. Besides, lithium iron phosphate and manganese spinel are also identified as cathode materials with great potential for applications. As an important component of the new generation of rechargeable LIBs, graphite served as the anode material and was used widely due to its unique hierarchical structure. In recent years, many high-performance anode materials have also been developed for the new generation of LIBs, including alloy materials and silicon-carbon-composites. Although the research on the cathode/anode materials of LIBs has attracted extensive interest, the deep understanding on their structural properties and the insight into the origin of structural formation are still lacking. For instance, rechargeable LIBs are currently facing the capacity degradation problem caused by the lithium plating, the formation of solid electrolyte interphase (SEI), the degradation of active substances in electrodes and the decomposition of electrolyte during the cycles. Therefore, it is very important to study the electrochemical reaction and lithium-ion transport process during the charging/discharging process of LIBs. Neutron, as an excellent probe to study the microstructure of materials, can play an important role in this research field.

James Chadwick first discovered the existence of neutrons through particle bombardment experiments and was awarded the Nobel Prize in Physics in 1935 for this discovery [10]. In the 1940s, Wollan et al. [11] completed neutron diffraction experiments at the Graphite Reactor in Oak Ridge National Laboratory, USA. Scattering theory explains well the interaction between neutrons and materials [12]. Neutron diffraction with a de Broglie wavelength of about 1 Å passing through crystalline material is one of the important approaches to study the periodic arrangement of the atoms inside the material. For magnetic materials, the neutron diffraction technique can also be used to determine their magnetic structure and to clarify their magnetic ground state with various spin configurations. Because the neutron scattering cross section is associated to the Fourier transform of the spatial correlation function, the reciprocal relationship exists between the characteristic real space distances and the scattering vector $Q = 4\pi sin(\theta)/\lambda$. Therefore, the primary task of the neutron diffraction measurement is to obtain the scattering vector dependence of neutron diffraction intensity, which is proportional to the scattering cross section. Given the fact that the lattice of crystalline materials exhibits periodicity, Bragg peaks appear at diffraction angles given by the Bragg equation $2dsin(\theta) = n\lambda$ during the neutron diffraction experiment. The integrated neutron diffraction intensity of the Bragg peaks is governed by the periodic arrangement of the atoms in the unit cell and the scattering from the atoms in the lattice of materials. That is to say, the detailed crystal structure information can be deduced by collecting a series of scattered intensities for many Bragg peaks at a neutron diffractometer, modeling the atomic structure and refining the parameters in order to get a satisfied agreement between calculated and observed intensities. For the collected neutron diffraction data, refinement can be performed when an initial structure model is known by methods such as Rietveld structure refinement [13–15]. Generally, Rietveld refinement can be done by computer programs, and the commonly used programs include GSAS [16], FullProf [17], TOPAS [18], RIETAN [19,20], etc.

In comparison with X-ray diffraction (XRD) or electron diffraction (ED), neutron powder diffraction (NPD) technique possesses many advantages in probing the microstructure of materials. For instance, NPD is more penetrating than XRD because it is based on the interaction of neutrons with the nuclei of atoms. Neutrons are free of charge and are therefore almost nondestructive to materials. The scattering length of neutrons is not proportional to their atomic number in the periodic table which makes elemental identification easier than other micro-probes, especially for light elements or elements with similar atomic masses. Neutrons have an intrinsic magnetic moment, which can provide insight into both crystal and magnetic structures of materials. Moreover, thermal neutrons possess characteristic wavelength which is comparable to spatial scale of atomic structure of condensed matter, resulting in prominent applicability and high accuracy in structural determination. In view of many advantages of NPD, more and more researchers are using this technology to characterize LIBs, which can be seen from the trend of the number of articles generated by neutron diffraction applied to LIBs in the past decades.

As the number of neutron sources and intense sources increased over time, the speed and quality of data collection improved significantly [21]. The well-known and cutting-edge spallation neutron sources in the world are SNS in the United States, J-PARC in Japan, ISIS in the United Kingdom and CSNS in China. Neutrons are also used in many other technologies, such as neutron depth profiling, neutron reflectometry, neutron imaging, total neutron scattering, neutron reflectometry, small angle neutron scattering, and incoherent neutron scattering, which can be used to study surface, bulk structure, and morphological changes in battery materials [22]. In present work, we summarize the applications of NPD technique in characterizing LIBs materials as well as the full cell. Since the elementary introduction and derivation of scattering theory can be found in many textbooks, we will skip basis principles and focus mainly on the application aspects.

2. Insight into the structural details in cathode materials

In recent decades, the study of the structural details in cathode materials plays a key role in promoting the performance of LIBs. Before the application of neutron diffraction, structural analysis was mostly completed by X-ray, electron beam and so on. By performing NPD experiments and taking advantages of this technique, more accurate structural information can be obtained for various electrode materials.

For most cathode materials, it is difficult to identify the light atoms (Li, O, F, et al.) with the existence of TM ions (Ni, Co, Mn, et al.) via XRD technique. Since neutron has high sensitivity to light elements, it is the method of choice to probe and deduce the accurate structural information of electrode materials for LIBs. It is well known that Li/Ni disordering has great influence on the properties of layered cathode materials, especially in Ni-rich cathode materials [23]. In the results of XRD, the diffraction signal from Ni is heavily stronger than that from Li, which will bring large error in quantifying the Li/Ni disordering. Therefore, for better understanding of the underlying mechanism of the effect, it is vital to obtain the exact Li/Ni disordering amount of the cathodes. Zhao et al. [24] employed neutron diffraction and refined the data by the Rietveld method via the Fullprof Suite to determine the degree of Li/Ni disordering. They synthesized $LiMn_{1/3}Ni_{1/3}Co_{1/3}O_2$ materials by co-precipitation and solid-state reaction. The results showed that the former presented less exchange between Li and Ni sites (Fig. 1a) and delivered better performance in electrochemical measurements. Similarly, for the recently focused Ni-rich layered cathodes family, Li/Ni disordering degree would also be obtained by NPD [25]. Additionally, other types of point defects could be quantified by NPD as well, such as the Li/Mn exchange in non-stoichiometric spinel-type $Li_{1+x}Mn_{2-x}O_4$ materials [26]. In these studies, NPD assisted in revealing the relationship between defects and electrochemical performance in cathode materials, which acted as guidance for the development of high-performance cathode materials.

Besides, to clarify the positions and occupancies of different atoms in cathode materials is also very important since the occupancies of lithium and oxygen in lattice will inevitably affect the diffusion of Li^+ and the stability of structure [27,28]. With the assistance of neutron, there is priority to reveal the occupancies of light atoms especially, such as lithium, oxygen and some doped atoms. For example, in pyrophosphate $Li_2FeP_2O_7$ cathode materials, the structure and transport properties have attracted much attention. Clark et al. [29] used neutron combined with advanced simulation to investigate diffusion pathways and activation

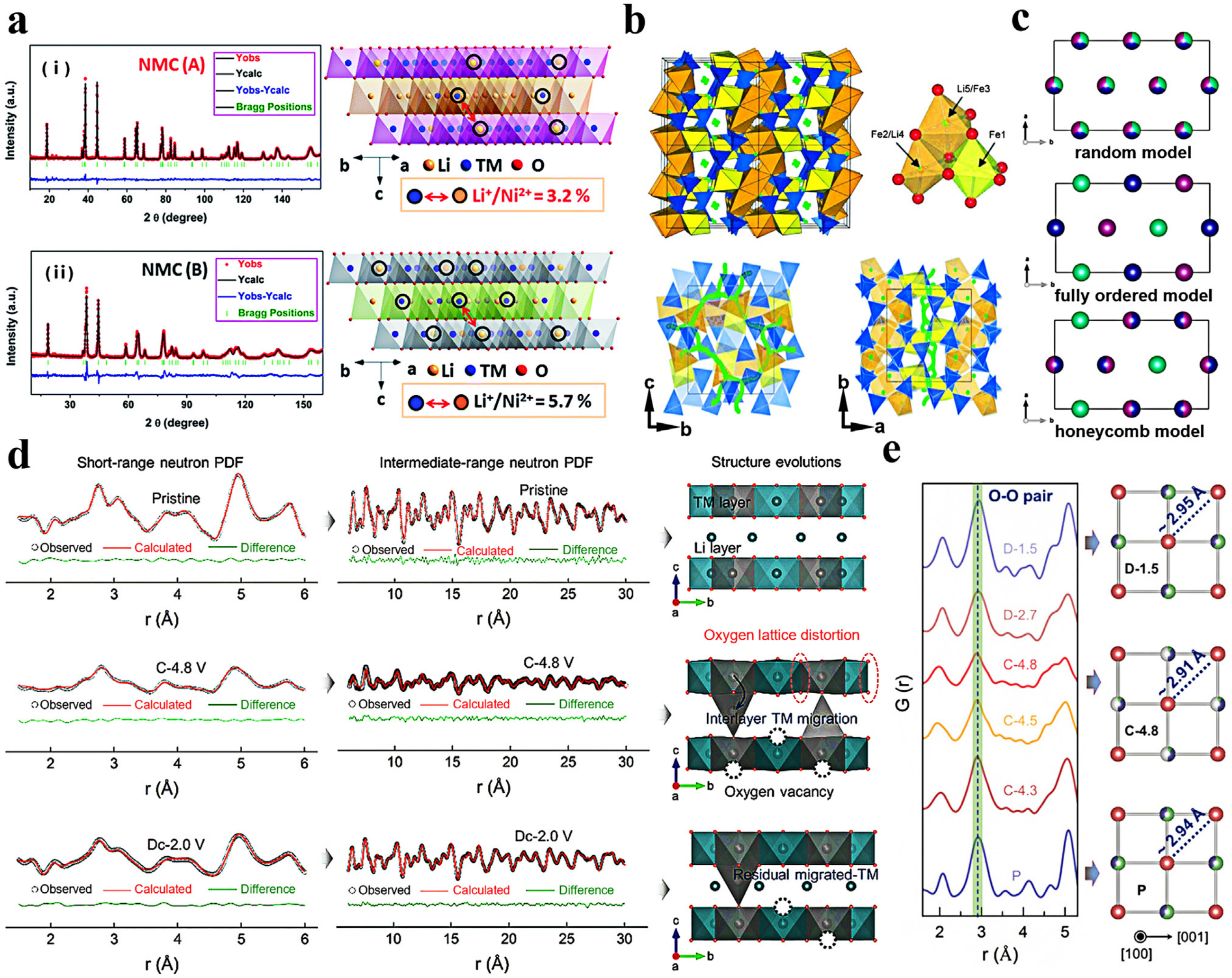

Fig. 1. (a) Rietveld refinement results of neutron diffraction patterns and illustration of crystal structures of (i) NMC (A) and (ii) NMC (B). Reprinted with permission from Ref. [24]. Copyright 2017, Royal Society of Chemistry. (b) Top: crystal structure of $Li_2FeP_2O_7$ is composed of Li ions (green), FeO_6 octahedral (yellow), mixed-occupancy FeO_5/LiO_5 units (orange), and P_2O_7 pyrophosphate (blue); Bottom: simulated "wavelike" trajectories of long-range Li $^+$ migration along projection of *bc*- and *ab*-plane, respectively. Reprinted with permission from Ref. [29]. Copyright 2012, John Wiley and Sons. (c) Different models established for the distribution of TM cation within the TM layers of $LiMn_{1/3}Ni_{1/3}Co_{1/3}O_2$, where Ni^{2+}, Mn^{4+} and Co^{3+} are drawn as spheres colored in green, purple and blue, respectively. Reprinted with permission from Ref. [35]. Copyright 2017, Cambridge University Press. (d) The short-range (local) and the intermediate-range neutron PDF data of the LR-NMC sample collected in different charging and discharging states. Reprinted with permission from Ref. [36]. Copyright 2022, John Wiley and Sons. (e) The local nPDF patterns and variation of the average O–O distance in $Li_{1.2}Ti_{0.35}Ni_{0.35}Nb_{0.1}O_{1.8}F_{0.2}$. Copyright 2019, John Wiley and Sons.

energies for Li^+ transportation. The refinement results of neutron diffraction patterns reveal that each of the polyhedral units share corners or edges to form a three-dimensional framework structure, where Li atoms occupy five sites forming distorted LiO_4 tetrahedra or distorted LiO_5 trigonal-bipyramids and Fe atoms occupy three sites forming FeO_6 octahedra or distorted FeO_5 trigonal-bipyramids (Fig. 1b). On this basis, the authors simulate the path way of lithium ions diffusion. They reveal curvilinear paths between adjacent Li sites (Fig. 1b), which generate "wave-like" trajectories for remote migration. This was subsequently confirmed by neutron diffraction maximum entropy analysis [30]. Additionally, for doping ions NPD can also deliver detailed occupational information. Fluorine substitution is a kind of anion doping, which can stabilize the structures of cathode materials [31,32]. Through NPD experiments, the occupancy of doped F ions can be precisely determined. There are research works showing that the presence of F in the $LiNi_{0.85}Co_{0.075}Mn_{0.075}O_2$ cathode materials increases the stability of electrode by forming a more stable local octahedron of halide [31]. In Li-rich cathode materials, anions framework in the F-doped cathode materials is very robust during charge and discharge processes [32].

The distribution of TM ions in cathode materials has a significant effect on electrochemical performance. Usually, the disordered phase (space group $Fd\bar{3}m$) of spinel $LiNi_{0.5}Mn_{1.5}O_4$ presents a higher capacity than the ordered phase (space group $P4_332$) [33]. However, it is difficult to distinguish the distribution of TM ions via XRD because of the limitation of X-ray. In contrast, one of the advantages of NPD is the capability of distinguishing adjacent TM ions. Recently, many studies have successfully revealed the ion arrangement in TM layers with the assistance of NPD [34,35]. Reynaud et al. [35] established three models of cation distribution in TM slabs for $LiMn_{1/3}Ni_{1/3}Co_{1/3}O_2$ via the program FAULTS (Fig. 1c), and then simulated the XRD, NPD and ED patterns of the three models. Results in XRD patterns showed that reflections in the 2θ *region* from 20° to 35° indexed for the new superstructure are so weak that they will probably be hidden in the background signal. In comparison, intensity of those in NPD patterns had noticeable differences to distinguish different structures. Therefore, one can identify the fully ordered model with a higher intensity of the superstructure reflections than the honeycomb model if the ordered TM distribution exists in the layered structure.

Except that the long-range structures could affect the performance of cathode materials, some short-range structures might also play a key role in their properties. One of the most important issues in Li-rich cathode materials is the occurrence of anion redox which is associated with the change of local structure. Zhao et al. [36] used neutron diffraction and pair distribution function (PDF) techniques to characterize the structure of $Li_{1.2}Ni_{0.13}Mn_{0.54}Co_{0.13}O_2$. It is found that the refined short-range PDF data are consistent with the stoichiometric ratio of the sample, which is suitable for quantitatively characterizing the local structure of the sample. As shown in Fig. 1d, by analyzing the neutron PDF data at different charged and discharged states, it is found that the oxygen lattice distorts at different states. Analysis of short-range neutron PDF data reveals that 14% of TM ions migrate from the octahedral sites in TM layers to the tetrahedral sites in Li layers. From another aspect, the distance of O–O pair can be directly displayed by neutron PDF measurement, which can also reflect the variation of lattice oxygen (Fig. 1e) [37]. In certain cathode materials, the existence of superstructure or local distortion can also be observed. In Na^+ and F^- co-doped layered NCM materials, most of the Bragg reflections of NPD pattern can be indexed properly with the $R\bar{3}m$ space group with a layered α-$NaFeO_2$ structure, except that some reflections at d spacing about 3.82 and 4.18 Å represent the formation of superstructure related to cation disordering [38]. In spinel Li_2MnO_3, the Jahn-Teller distortion can be detected easily via NPD technique which can lower the symmetry of the crystal structure from cubic to tetragonal [39], leading to the degradation of electrochemical performance of the cathode materials. Obviously, with the assistance of neutron diffraction technique, structural details of various cathode materials can be obtained, which will be beneficial to construct structure-activity relationship and to design high performance cathode materials.

3. Insight into the structural details in anode materials

As mentioned above, the safety and stability of the LIBs cathode material is a crucial factor. Likewise, as an important component of LIBs, the performance of the anode cannot be ignored. Among all anode materials, graphite anode has been developed for several decades and has been applied widely in the battery market. The safety of the graphite anode is intimately related to the de-intercalation of lithium ions. Given the fact that the typical LIBs are independent devices isolated from the outside world and the structural change of anodes takes place immediately upon charging and discharging, it is challenging to study the intercalation and deintercalation processes of lithium ions in anodes. Neutron diffraction is a non-destructive technique and can also give accurate information about the occupancy of different lithium sites in the anode materials with different degrees of lithium removal. Hence, it can be applied to solve specifically the structural issues in graphite anode.

Senyshyn et al. [40] have used spatially-resolved monochromatic neutron diffraction to indicate that there is a heterogeneous distribution of lithium in the fresh state of 18650-type cells. His research group found that lithiation level in fatigue batteries is basically low, and the homogeneity of the lithium concentration is further decreased, which will undoubtedly have an impact on the stability and safety of LIBs [41]. To further explore the heterogeneous distribution of lithium ions, his group [42] divided the 18650 batteries into four groups: fresh batteries and batteries that respectively cycled 120, 210 and 400 times at ambient temperature using currents that were set close to the specified maximum of C/2 for charge and 2C for discharge. It was found that the capacity of the batteries decreased significantly with the increase of the cycle number. The authors used monochromatic neutron diffraction to probe the four groups of cells. They found that the LiC_{12}/LiC_6 ratio of the lithium intercalated graphite changed with the increase of the cycle number, which indicated that the loss of movable lithium was directly related to the decline of the capacity in the batteries. The two-dimensional distribution of the lithium concentration in the lithiated graphite anode Li_xC_6 was obtained by spatially-resolved time-of-flight (TOF) NPD. As shown in Fig. 2a, the lithium distribution in fresh batteries is quasi-uniform within the standard deviations, and all integral characteristics, including average lithium concentration $<x_{Li}>$ as well as its deviation from constant, median of the distribution and the plateau value x_p, reduce to different degrees upon cycling. The NPD has also been applied to study 26650-type LIBs [43]. The *ex situ* NPD data revealed that milder charge conditions lead to higher reflection intensities of lithiated graphite and harsher conditions reduce reflection intensity, as shown in Fig. 2b. In other words, under the same state of charge, the milder the conditions, the more the graphite electrode has transformed to LiC_{12}. More importantly, this work is very important to solve the problem of the heterogeneity, safety and stability of the LIBs anode.

In addition to the graphite anode, some other anode materials also show their special properties. Because of the zero-strain characteristic, anode material $Li_4Ti_5O_{12}$ has also attracted researchers' interests. However, the mechanism of the phase transition that occurs during the reaction is still not well understood, and such small changes can affect the performance of the $Li_4Ti_5O_{12}$ anodes. From the Rietveld refinement of NPD data of $Li_4Ti_5O_{12}$, researchers described the position of Li in 8*a* and 16*c* sites, as shown in Fig. 2c [44]. Upon charging, the insertion sites of Li will be influenced by O position. So, in order to gain the exact position of Li, they refined the O position earlier, then deduced the accurate structure and formula of compound as $Li^{8a}{}_{0.46(26)}Li^{16c}{}_{1.20(23)}(Li_{1/3}Ti_{5/3})^{16d}O^{32e}{}_4$. This work revealed the underlying mechanism for particle-size-induced changes in battery performance. Likewise, as an anode material, the mixed oxide $TiNb_2O_7$ was proved to be a promising candidate because of its high capacity. However, the understanding of atomistic mechanisms underlying the lithiation reaction is limited, which is not conducive to the application and promotion of the material. The TOF NPD is employed to study the structure and lithium atoms distribution of $TiNb_2O_7$ [45]. The refinement results show that there are two kinds of insertion sites in $TiNb_2O_7$, i.e. fivefold- and fourfold-coordinated sites. Although inserting into fivefold-coordinated sites needs less energy, Li atoms randomly insert between the two sites, which suggests that lithium insertion into $TiNb_2O_7$ is driven by the entropy increase dominantly. Because NPD is more sensitive to light elements, compared with XRD, it can give more accurate information about lithium ions in the crystal lattice. NPD was again proved to be an excellent tool for the study of electrode materials for LIBs.

4. Clarification of the structural evolution of electrodes in LIBs

4.1. Structural evolution in cathode materials

Upon charging or discharging, the crystal structure of electrode materials in LIBs will inevitably change accompanied with the diffusion of lithium ions. Therefore, to study the structural evolution of electrode materials at different charging states is helpful to understand the charging mechanism. The structure of electrode materials is generally in metastable state during charge and discharge. When the voltage is withdrawn, the structure will slowly recover partially. In addition, metastable structures and other components of the battery, such as the electrolyte, are often sensitive to air and humidity. Therefore, the *ex-situ* structure analysis technique cannot accurately reflect the evolution of the structure, and the *in operando* measurement technique becomes an urgent need for the research of LIBs.

As three distinct TM elements play different roles in $Li(Ni_xMn_yCo_z)O_2$ $(x+y+z=1)$ [46], they are rapidly developing in energy storage systems and power batteries. Therefore, it is very important to clarify the role of each element. Goonetilleke et al. [47] used *in operando* neutron diffraction to elucidate the influencing factors of the structural evolution in $Li(Ni_xMn_yCo_z)O_2$ $(x + y + z = 1)$ cathode materials. It is found that the stability and electrochemical properties of the cathode materials are related to the composition of TMs when working in a wide charge-discharge window. Fig. 3a shows contour plots of diffraction pattern for NMC541 as a function of time. NMC811 showed the largest

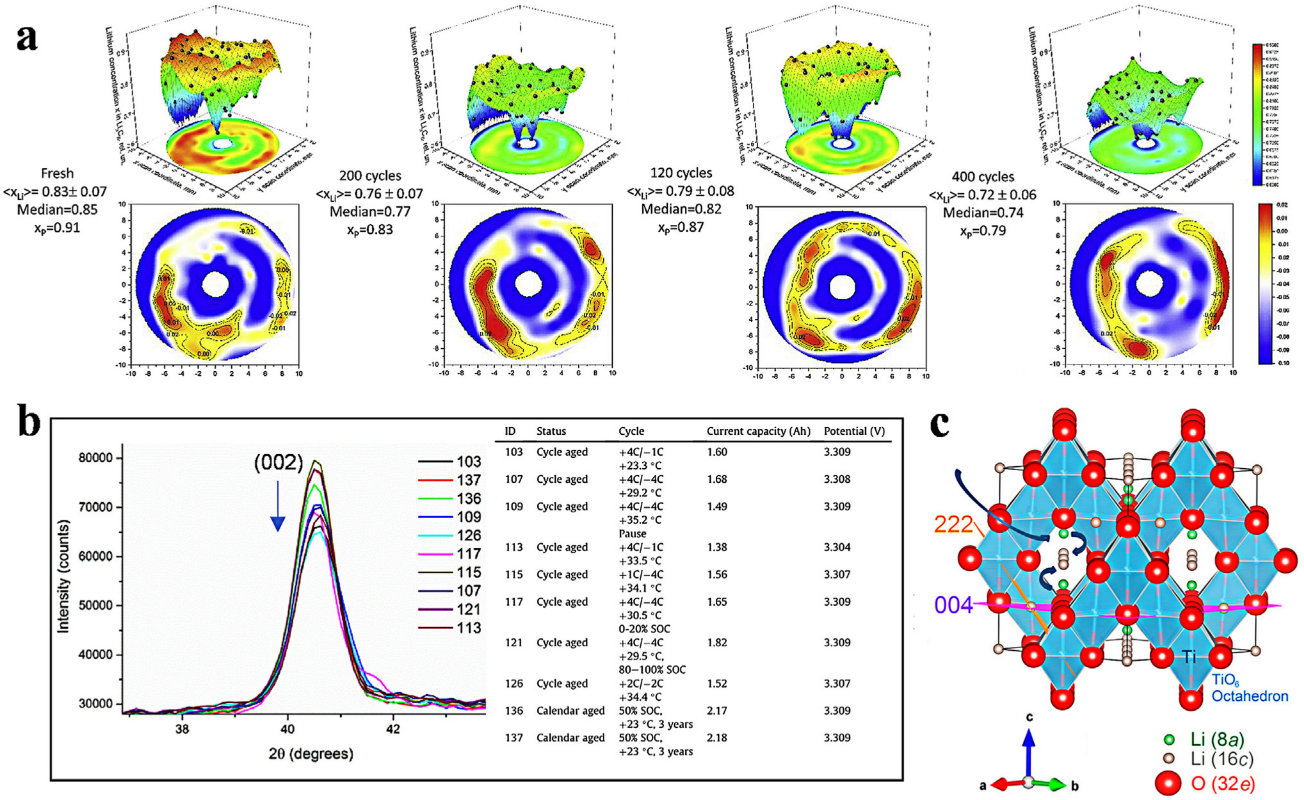

ID	Status	Cycle	Current capacity (Ah)	Potential (V)
103	Cycle aged	+4C/−1C +23.3 °C	1.60	3.309
107	Cycle aged	+4C/−4C +29.2 °C	1.68	3.308
109	Cycle aged	+4C/−4C +35.2 °C Pause	1.49	3.309
113	Cycle aged	+4C/−1C +33.5 °C	1.38	3.304
115	Cycle aged	+1C/−4C +34.1 °C	1.56	3.307
117	Cycle aged	+4C/−4C +30.5 °C 0-20% SOC	1.65	3.309
121	Cycle aged	+4C/−4C +29.5 °C, 80−100% SOC	1.82	3.309
126	Cycle aged	+2C/−2C +34.4 °C	1.52	3.307
136	Calendar aged	50% SOC, +23 °C, 3 years	2.17	3.309
137	Calendar aged	50% SOC, +23 °C, 3 years	2.18	3.309

Fig. 2. (a) Experimental lithium distribution *vs.* cycle number for cylinder-type LIBs with different cycles as derived from time-of-flight neutron diffraction. The first row, second row, and third row of text are integral characteristics of lithium distribution, in-plane lithium distribution and deviations of lithium distribution from plateau value x_p. Reprinted with permission from Ref. [42]. Copyright 2020, Elsevier. (b) Different 2θ regions with highlighting the graphite-type reflections are shown, based on the *ex situ* NPD data of 26650 batteries aged under the conditions that listed the table on the right. Reprinted with permission from Ref. [43]. Copyright 2017, Elsevier. (c) Crystal structure of $Li_{4+z}Ti_5O_{12}$ with the (222) and (004) planes indicated. The dark blue arrows indicate the theoretical pathway of Li (inward) diffusion during lithiation. Reprinted with permission from Ref. [44]. Copyright 2014, American Chemical Society.

volume change per cell during cycling (6.97%) and the smallest volume in the charged state (93.4 Å^3), whereas NMC442 showed the smallest change in unit cell volume (3.36%) during the cycle. It can be concluded that in NCM cathode materials, the lattice volume changes during cycling tend to be larger with higher Ni content, while the lattice volume changes tend to be smaller with higher Mn and Co content. In addition, the relative ratio of volume shrinkage (normalized to the initial cell volume) for the measured NCM cathode materials, as shown in Fig. 3b, is regardless of the change in nickel content [48]. This implies there may be a general mechanism for the anisotropic volume change of nickel-rich positive electrodes. To a certain extent, it is also shown that the macroscopic strain/stress caused by cell volume collapse may follow a similar trend in the measured samples under the same degree of lithium removal.

The greater change of lattice parameters in the cycle process indicates the greater accumulation of mechanical repetitive stress, which often accelerates the destruction and failure of the cathode material structure [49, 50]. Wu et al. [51] explored the structural evolution of NCM622 positive electrode at different magnification rates of 0.27, 1.6, 2.4, 3.2 and 4.4 C via *in operando* neutron diffraction technique. As shown in Fig. 3c, the lattice parameters of NMC622 have similar trends at different charging rates. This indicates that the crystal structure of NMC622 is well maintained during fast charging, which is in line with previous reports of the excellent structure retention ability of NCM at a high rate up to 10C [52].

In the process of charging and discharging, the migration path of lithium ion is closely related to the diffusion coefficient of lithium ion, which is also very important for cathode materials [53–55]. It has been widely believed that lithium ions diffuse in layered NCM materials by oxygen dumbbell hopping (ODH) and tetrahedral site hopping (TSH) [56]. Our group [57] used *in operando* neutron diffraction and the maximum entropy method (MEM) to reveal a new migration path of lithium ions in the layered positive electrode under operating conditions, as shown in Fig. 3d. In the initial charging phase, lithium ions migrate through the TSH path, and with the gradual exit of lithium ions, the migration path starts to change into an unpredictable indirect zigzag jump (IZH) path. Finally, IZH path becomes the dominant migration path under high voltage condition. Along the IZH route, lithium ions migrate to adjacent vacancies via a curved path, passing through the center of the oxygen dumbbell on their way. And the change of the migration path from TSH to IZH is not conducive to maintaining the rapid diffusion of lithium ions during the charging process verified on the galvanostatic intermittent titration technique (GITT) curve. This work can enlighten us to design an optimized lithium ion migration path to obtain high-performance LIBs.

In operando neutron diffraction has been shown to have a sensitive ability to detect phase transitions and can be used to investigate real-time phase transitions during charging and discharging [58]. The *in operando* neutron diffraction is used to conduct charging and discharging test of LiNi0·5Mn1·5O4 (d-LNMO) at 0.05 C [59]. In the charging and discharging curve of the first cycle, three platforms are observed along with the $Ni^{2+} \rightarrow Ni^{4+}$ transition, accompanied by the shift of (222) Bragg peak toward high angle, indicating that a solution reaction has occurred, as shown in Fig. 3e. In addition, the Li-content-dependent phase evolution behavior in $Li_{1+x}Mn_{2-x}O_4$ ($x = 0$, 0.05, and 0.1) spinel-type cathodes was also investigated via *in operando* NPD [60]. The $Li_{1.1}Mn_2O_4$ cathode exhibits only solid-solution behavior. By contrast, $LiMn_2O_4$ shows a two-phase reaction mechanism and the phase evolution behavior of $Li_{1.05}Mn_2O_4$ falls in a combination of solid solution and first order phase transition. Correlating the phase transitions to the electrochemical charge/discharge curves indicates that the initial composition of the electrode materials has a significant

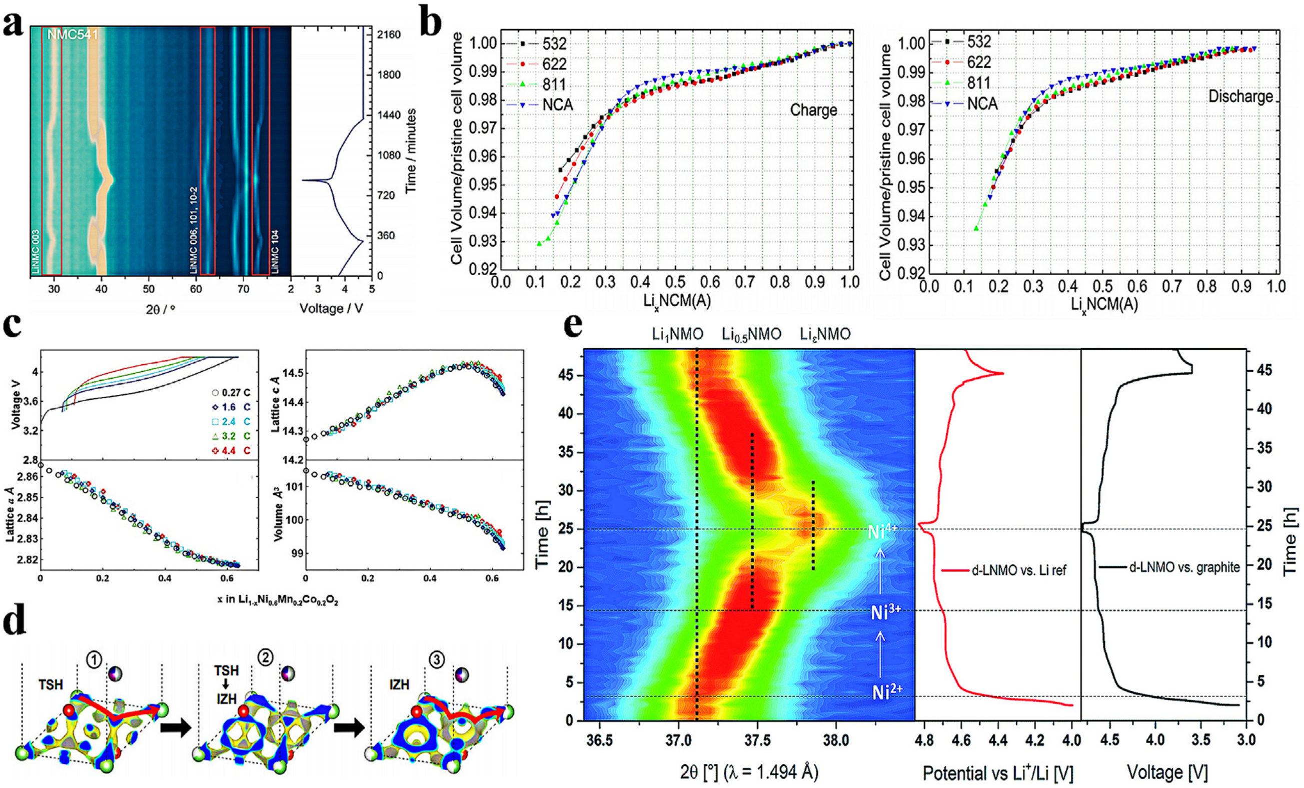

Fig. 3. (a) Contour plots of NMC541 with intensity shown increasing from the darkest to the lightest of the diffraction patterns as a function of time. Reprinted with permission from Ref. [47]. Copyright 2019, American Chemical Society. (b) Normalized cell volume evolution during the initial charge and discharge of different NMC compositions and NCA. Reprinted with permission from Ref. [48]. Copyright 2021, Royal Society of Chemistry. (c) Lattice parameter evolution for NMC622 under different charging rates. Reprinted with permission from Ref. [51]. Reprinted under terms of the CC-BY license. (d) MEM reconstructed negative nuclear density maps for NCM523 at different charge states based on *in operando* neutron diffraction data. Reprinted with permission from Ref. [57]. Copyright 2022, Elsevier. (e) Contour plot representation of an *operando* NPD measurement of the first cycle of the d-LNMO *vs.* graphite cylindrical cell: (left) the (222) d-LNMO reflection is plotted; (right) the galvanostatic cycle of d-LNMO *vs.* Li reference or *vs.* graphite. Reprinted with permission from Ref. [59]. Copyright 2017, Royal Society of Chemistry.

influence on phase evolution and determines the electrochemical performance. Similarly, for LFP cathode materials, the phase transition in the dehydrogenation process can be carried out through solid solution reaction or two-phase reaction, which is mainly affected by sample preparation and electrochemical conditions [61]. Goonetilleke et al. [62] studied the changes in the structure of Mg-doped $LiFePO_4$ during charge-discharge processes at different temperatures. This kind of doping does not affect the reaction mechanism of the material in the cycling process, and evidence of two reactions is observed in the diffraction data, as shown in Fig. 4a. The reflection peaks corresponding to lithiated $Li(MgFe)PO_4$ phase and delithiated $(MgFe)PO_4$ phase appear and disappear alternately, indicating that the transition between these two phases occurs during battery charging and discharging. The subsequent electrochemical data proved that, although the reaction kinetics of $Li(MgFe)PO_4$ material is faster at higher temperature, the reaction mechanism and structural polarization are temperature invariant.

Generally, the cathode materials are fabricated via different approaches containing sintering procedure at high temperature. During the heating process, the structure of cathode material is generally metastable. When the temperature decreases, its structure will slowly recover. The *in situ* neutron diffraction technology during the heating process can just be used as a method to analyze the dynamic changes of its structure. Our group [63] used *in situ* and *ex situ* NPD to investigate the phase structural evolution of $LiNi_{0.8}Co_{0.1}Mn_{0.1}O_2$ (NCM811) cathodes at 600, 700, 800, 900 and 1000 °C, as shown in Fig. 4b. The results show that when treated at 400 °C, NCM811 can recover from the disordered structure and has an optimized surface morphology, thus improving the electrochemical behavior. Heat treatment of NCM811 at higher temperature induces a layered-to-rock-salt structure transition accompanied with the precipitation of lithium oxide. Therefore, low temperature reheating may be a simple and useful method to improve the properties of lamellar cathode materials. Meanwhile, *in situ* neutron diffraction and PDF are used to reveal the mechanism of $LiNi_{0.5}Mn_{1.5}O_4$ spinel structure instability under the annealing at the oxygen-deficient atmosphere (Fig. 4c) [64]. It is found that the lack of oxygen reduces the Mn valence from +4 to +3 at 650 °C, disordering the Ni/Mn rearrangement at relatively low temperature, and promotes the formation of the layered rock-salt (LRS) phase by Ni segregation. At the same time, the transition of the LRS phase generated by TM migration is triggered to fill the octahedral interstitial positions of the oxygen sublattice. Upon heating, TM migration and exchange with Li in residual spinel and newly formed LRS exhibit a multistage behavior.

4.2. *Structural evolution in anode materials*

The anode material of LIBs with large reversible ion storage capacity and good stability must have sufficient space for ion storage and transport in the structure, as well as the ability to maintain structural stability during the repeated intercalation/deintercalation of ions. The lack of structural revolution information gained from *ex situ* neutron characterization in real charging and discharging process prevents researchers from understanding the structural evolution. The development of *in operando* neutron diffraction techniques possesses prominent ability to solve this problem.

It is known that the lithiation and delithiation reactions in rechargeable LIBs are often accompanied by multi-stage phase transition reactions and structural changes, such as graphite anodes that may undergo phase structures like LiC_{12} before the final formation of LiC_6 [65–68]. *In operando* NPD holds the high sensitivity to light elements such as lithium and carbon of electrochemical species, and thus can well characterize this kind of phase change reactions [37,69]. With the help of

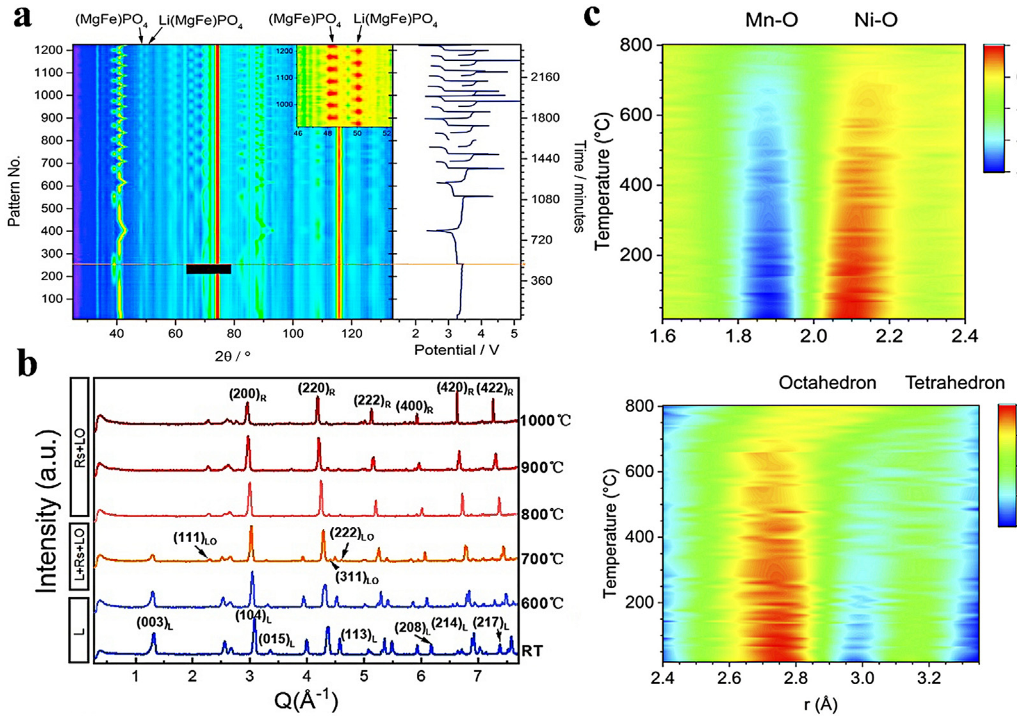

Fig. 4. (a) *In operando* NPD diffraction data for batteries cycled at 323 K. Reprinted with permission from Ref. [62]. Copyright 2018, Elsevier. (b) *In situ* NPD patterns of NCM811 cathode materials treated at different temperatures. Reprinted with permission from Ref. [63]. Copyright 2020, Elsevier. (c) *In situ* PDF of $LiNi_{0.5}Mn_{1.5}O_4$ during the continuous heating (Top: contour plot of Mn–O (r ~ 1.88 Å) and Ni–O (r ~ 2.1 Å) correlations; Bottom: contour plot of the correlations of the octahedral (r ~ 2.7 Å) and tetrahedral (r ~ 3.15 Å) oxygen cages). Reprinted with permission from Ref. [64]. Copyright 2022, Elsevier.

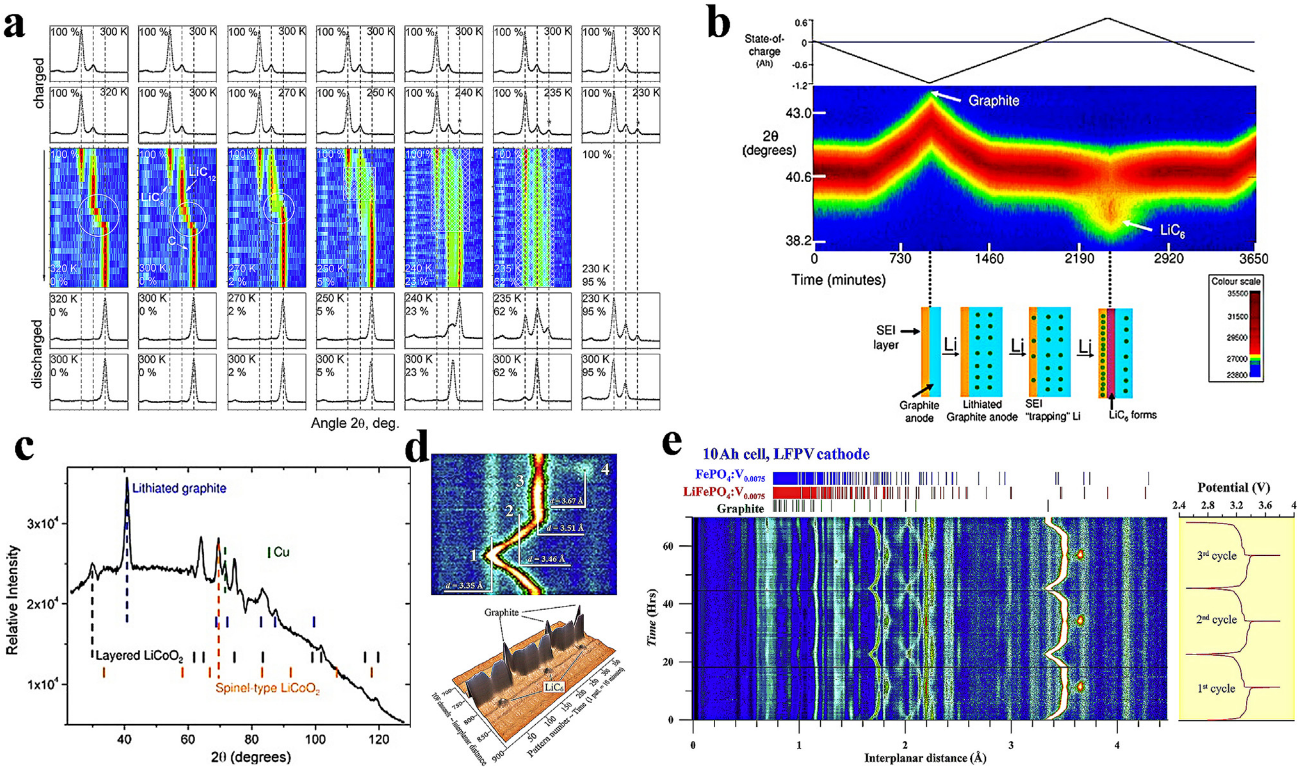

Fig. 5. (a) The enlarged section of neutron diffraction patterns collected in charged and discharged states at different temperatures (anodes of 18650 e type commercial LIBs). Reprinted with permission from Ref. [71]. Copyright 2015, Elsevier. (b) Neutron diffraction patterns collected from graphite anode material of commercial $LiCoO_2$/graphite cells [65]. (c) Neutron diffraction patterns of graphite in charged state. Reprinted with permission from Ref. [65]. Copyright 2010, Elsevier. (d) Enlarged 2D diffraction pattern and 3D visualization of diffraction peak in LFP-battery anode. Reprinted with permission from Ref. [73]. Copyright 2014, Elsevier. (e) Diffraction patterns of a vanadium-doped LFP-battery. Reprinted with permission from Ref. [73]. Copyright 2014, Elsevier.

in operando NPD techniques, the intercalation of lithium into the lattice structure of graphite structure is generally considered as a reaction that proceeds in steps [70–72]. By tracing the formation of multiple LiC$_x$ phases during the multi-stage reaction of lithium insertion into graphite anode materials and the redistribution of lithium in the graphite structural matrix during charge and discharge processes via NPD, the changes in the structure and composition during the intercalation process are well characterized, as shown in Fig. 5a. The temperature-driven discontinuity in the phase transition and the anomalous behavior of LiC$_6$ suggest a possible change in the thermodynamic stability range of the graphite anode at low temperatures. During the phase transformation of lithiated graphite, there may be cases where both phases are present and lithium ions accumulate near the anode surface or in the SEI layer in the charging state [65], as shown in Fig. 5b and c. Bobrikov et al. [73] traced the formation of multiple LiC$_x$ phases during the multi-stage reaction of lithium insertion into graphite anode materials and the redistribution of lithium in the graphite structural matrix accompanied by gradual changes in the distance between carbon layers during charging and discharging by NPD, as shown in Fig. 5d and e. What is more, the structural phase change of the lithiation-delithiation reaction occurring in the graphite anode is not completely reversible in a full-cell system consisting of a spinel lithium-manganese oxide cathode and a graphite anode during electrochemical cycling. The content of the LiC$_{12}$ phase is different with the increase of the number of electrochemical cycles [74].

Lithium plating generally refers to the situation where lithium ions are reduced to lithium metal on the anode side, rather than being embedded in the anode crystal structure [75]. The reason for the deposition of metallic Li on the anode is that the potential of lithium intercalation into graphite is close to the potential difference of Li/Li$^+$ [76,77]. Lithium deposited on the cathode material may lead to the formation of lithium dendrites, which may cause serious consequences such as short circuits in LIBs. By comparing the reflection intensity of *in operando* NPD patterns of LiC$_x$ obtained from the lithiation reaction at different charge rates [77,78], it is tentatively concluded that only a partial phase transition occurs in the deposited graphite of lithium, and the amount of lithium corresponding to the charge capacity is not fully embedded in the main structure. The result shows that at this charging range a limitation in electrolyte potential, diffusivity and electrode kinetics [79] leads to the reaction of lithium plating as secondary side reactions. The extent of the lithium plating reaction, which is a competing reaction against the reaction of lithium intercalation in graphite, diminishes due to the decrease in current.

5. Perspective of the application of neutron diffraction technique

The general applications of neutron diffraction technique in studying the structural properties of cathode and anode materials are summarized

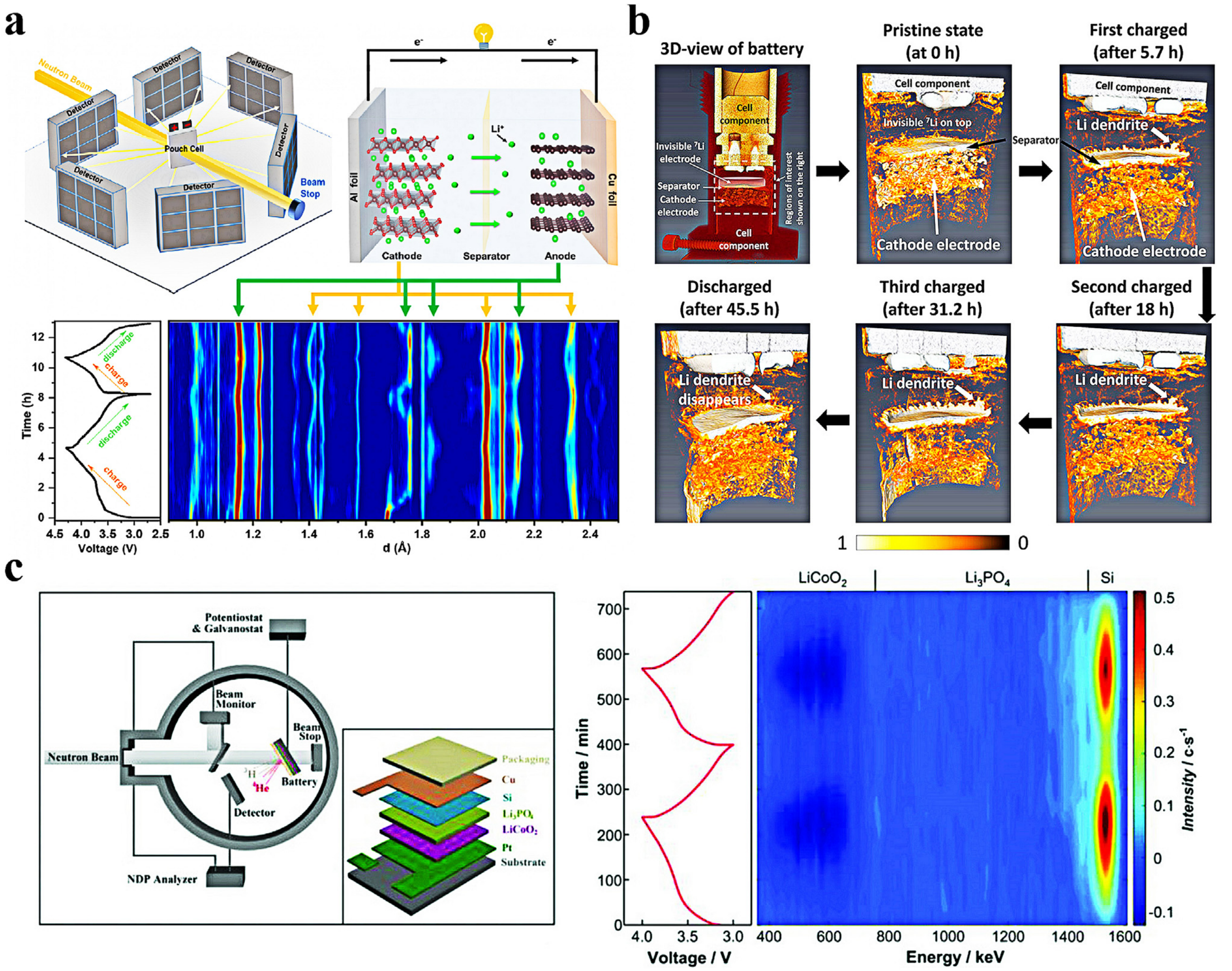

Fig. 6. (a) *In operando* neutron diffraction study on NCM523/graphite full cell. Reprinted with permission from Ref. [57]. Copyright 2022, Royal Society of Chemistry. (b) Three-dimension evolution of the Li distribution in the cells at different stages of charging and discharging. The contrast value from 0 to 1 represents an increased trend of absorption of neutrons. Reprinted with permission from Ref. [83]. Copyright 2019, Royal Society of Chemistry. (c) From the left to right are the models of the NDP set-up, the *in operando* spatial difference energy spectra during the first two charging and discharging cycles. Reprinted with permission from Ref. [84]. Copyright 2018, Royal Society of Chemistry.

above. Most of the neutron diffraction works were performed in *ex situ* mode, whereas the *in operando* measurement is essential to get insight into the structural evolution and structural degradation associated directly with the electrochemical performance of electrodes. Obviously, obtaining the information of full cell under real operating conditions is essential for the research and development of metal ion batteries. For the full cell, its degradation mechanism is often caused by the synergistic action of both cathodes and anodes. With the strong penetrating power of neutrons, it is possible to analyze the distribution of lithium inside LIBs nondestructively under working conditions. Therefore, it is especially beneficial to understand the failure mechanism via neutron technology. It is demonstrated that the degradation of the cell is possibly inhomogeneous [80], and the electrodes near the center work better than those near the edges. What is more, *in operando* NPD study shows that the aging of cells during cycling is related to the structural failure of anode and cathode material [81]. The reduction of active lithium in cells would also have a great impact on the degradation behavior of batteries after a long-time cycle. Our group [57] found that in the full battery composed of NCM523 cathode and graphite anode, 52.8% of lithium-ions was released from NCM523 in the charging state of the first cycle (Fig. 6a), indicating that there is still a lot of space to improve the energy density of NCM523 in the full cell. Small amounts of lithium-ions (~4.3%) that are not inserted back are retained in graphite as $Li_{1-x}C_{18}$ and $Li_{1-x}C_{54}$, or consumed during the formation of SEI. Besides, most neutron researches on full cells are carried out on cells with relatively small capacity, but even for LIBs with larger capacity, whose initial capacity is 15 Ah or even up to 50 Ah, neutron diffraction technique would also be applied and probe the microstructure of them handily [82].

It is worth noting that some other neutron techniques besides NPD could also play an important role in understanding the working mechanism of LIBs. For example, by applying neutron imaging technology, researchers successfully observed that the lithium dendrite grows on the surface of lithium metal when the battery is charged and then disappears when the battery is discharged (Fig. 6b) [83]. Additionally, neutron depth profiling (NDP) technique is employed to investigate the all-solid-state, thin film Si–Li_3PO_4–$LiCoO_2$ batteries [84]. It is observed that the Li-immobilization layer exists between the anode and electrolyte, which could explain the degradation of the batteries (Fig. 6c). The uniform-distribution of lithium dendrites in the solid electrolyte can also be detected via NDP [85].

Accompanied with the advancement of neutron source and neutron instrumentation, extensive and specific application of neutron diffraction technique will certainly be employed in the near future for exploring more detailed structure information in LIBs. Especially, the *in operando* neutron diffraction technique will be employed routinely not only for studying cathode/anode materials in full cells, but also for studying solid state electrolyte materials in all-solid-state batteries, thus providing new perspectives in developing high performance LIBs.

6. Summary

In summary, this article reemphasizes that NPD is a well-established technique for characterizing LIBs based on the interaction between neutrons and atomic nuclei, and consequently it has more powerful penetrability than X-rays and sensitivity for light elements or elements with similar atomic masses. As the above-mentioned recent literatures clearly show, the structural details of electrode materials in LIBs can be explored by the methods of NPD, and the position as well as the occupancy of lithium elements in lithium-containing compounds can be accurately obtained. Current directions of application include the analysis of the presence of anti-site-defects and bond distances in the lattice structure of electrode materials, the analysis of the homogeneous or non-homogeneous distribution of lithium ions, and the analysis of the lithium ion intercalation selectivity. In addition, the design of *in operando* NPD experiments of LIBs under different charge and discharge states allows an in-depth analysis of the electrochemical reactions occurring in the batteries and the evolution of the structure during the dynamics processes. So far, *in operando* neutron diffraction technique has been used to characterize the lattice parameter changes and phase transition reactions of electrode materials in LIBs, the macroscopic strain/stress caused by the cell volume collapse, the migration path of Li ions during charge and discharge, and the degree of proceeding and reversibility of the reaction of Li-plating. With the development of neutron diffraction technology, NPD could be employed extensively in various battery systems and help analyzing complicated structural problems in LIBs, which will certainly provide beneficial guidance in developing new-generation high performance LIBs.

Declaration of competing interest

The authors declare that they have no known competing financial interests or personal relationships that could have appeared to influence the work reported in this paper.

Acknowledgements

The research was financially supported by National Key R&D Program of China (2020YFA0406203), National Natural Science Foundation of China (Nos. 52072008 and U2032167), Shenzhen Fundamental Research Program (No. GXWD 20201231165807007-20200807125314001), and Guangdong Basic and Applied Basic Research Foundation (No. 2022B1515120070).

References

[1] J.B. Goodenough, K.S. Park, The Li-ion rechargeable battery: A perspective, J. Am. Chem. Soc. 135 (2013) 1167–1176.
[2] G.N. Lewis, F.G. Keyes, The potential of the lithium electrode, J. Am. Chem. Soc. 35 (1913) 340–344.
[3] M.S. Whittingham, Lithium batteries and cathode materials, Chem. Rev. 104 (2004) 4271–4301.
[4] M. Li, J. Lu, Z. Chen, K. Amine, 30 Years of lithium-ion batteries, Adv. Mater. 30 (2018) 1800561.
[5] K. Mizushima, P.C. Jones, P.J. Wiseman, J.B. Goodenough, Li_xCoO_2 ($0 < x \leqslant 1$): A new cathode material for batteries of high energy density, Solid State Ionics 3–4 (1981) 171–174.
[6] D. Caurant, N. Baffier, B. Garcia, J.P. Pereira-Ramos, Synthesis by a soft chemistry route and characterization of $LiNi_xCo_{1-x}O_2$ ($0 \leqslant x \leqslant 1$) cathode materials, Solid State Ionics 91 (1996) 45–54.
[7] A. Rougier, I. Saadoune, P. Gravereau, P. Willmann, C. Delmasa, Effect of cobalt substitution on cationic distribution in $LiNi_{1-y}Co_yO_2$ electrode materials, Solid State Ionics 90 (1996) 83–90.
[8] Z. Lu, D.D. MacNeil, J.R. Dahn, Layered Li $[Ni_xCo_{1-2x}Mn_x]O_2$ cathode materials for lithium-ion batteries, Electrochem. Solid State Lett. 4 (2001) A200.
[9] D.D. MacNeil, Z. Lu, J.R. Dahn, Structure and electrochemistry of $Li[Ni_xCo_{1-2x}Mn_x]O_2$ ($0 \leqslant x \leqslant 1/2$), J. Electrochem. Soc. 149 (2002) A1332.
[10] J. Chadwick, Possible existence of a neutron, Nature 129 (1932) 312.
[11] W.L. Davidson, G.A. Morton, C.G. Shull, E.O. Wollan, Diffraction of neutrons by hydrogen and deuterium containing crystals, Phys. Rev. 72 (1947) 168–169.
[12] R.G. Newton, Scattering Theory of Waves and Particles, second ed., 1982.
[13] R.J. Hill, C.J. Howard, Quantitative phase-analysis from neutron powder diffraction data using the rietveld method, J. Appl. Crystallogr. 20 (1987) 467–474.
[14] L.B. McCusker, R.B. Von Dreele, D.E. Cox, D. Louer, P. Scardi, Rietveld refinement guidelines, J. Appl. Crystallogr. 32 (1999) 36–50.
[15] R.A. Young, D.B. Wiles, Profile shape functions in rietveld refinements, J. Appl. Crystallogr. 15 (1982) 430–438.
[16] B.H. Toby, R.B. Von Dreele, *GSAS-II*: The genesis of a modern open-source all purpose crystallography software package, J. Appl. Crystallogr. 46 (2013) 544–549.
[17] T. Ohzuku, Y. Iwakoshi, K. Sawai, Formation of lithium-graphite intercalation compounds in nonaqueous electrolytes and their application as a negative electrode for a lithium ion (shuttlecock) cell, J. Electrochem. Soc. 140 (1993) 2490–2498.
[18] A.A. Coelho, *TOPAS and TOPAS-Academic*: An optimization program integrating computer algebra and crystallographic objects written in C++, J. Appl. Crystallogr. 51 (2018) 210–218.
[19] F. Izumi, K. Momma, Three-dimensional visualization in powder diffraction, Appl. Crystallogr. 130 (2007) 15–20.
[20] Y.I. Kim, F. Izumi, Structure refinements with a new version of the rietveld-refinement program RIETAN, J. Ceram. Soc. Jpn. 102 (1994) 401–404.
[21] D. Goonetilleke, N. Sharma, *In situ* neutron powder diffraction studies, Phys. Sci. Rev. 6 (2021) 20180155.
[22] D. Liu, Z. Shadike, R. Lin, K. Qian, H. Li, K. Li, S. Wang, Q. Yu, M. Liu, S. Ganapathy, X. Qin, Q.-H. Yang, M. Wagemaker, F. Kang, X.-Q. Yang, B. Li, Review of recent

development of in situ/operando characterization techniques for lithium battery research, Adv. Mater. 31 (2019) 1806620.

[23] L.H. Liu, M.C. Li, L.H. Chu, B. Jiang, R.X. Lin, X.P. Zhu, G.Z. Cao, Layered ternary metal oxides: Performance degradation mechanisms as cathodes, and design strategies for high-performance batteries, Prog. Mater. Sci. 111 (2020) 100655.

[24] E. Zhao, L. Fang, M. Chen, D. Chen, Q. Huang, Z. Hu, Q. Yan, M. Wu, X. Xiao, New insight into Li/Ni disorder in layered cathode materials for lithium ion batteries: A joint study of neutron diffraction, electrochemical kinetic analysis and first-principles calculations, J. Mater. Chem. 5 (2017) 1679–1686.

[25] Y. Idemoto, Y. Tsukada, N. Kitamura, A. Hoshikawa, T. Ishigaki, Change in crystal structure of $LiNi_{0.8}Co_{0.19}Cu_{0.01}O_2$ cathode during charge of coin cell observed by ex situ time-of-flight neutron diffraction, Chem. Lett. 40 (2011) 168–170.

[26] R. Wang, X. Chen, Z. Huang, J. Yang, F. Liu, M. Chu, T. Liu, C. Wang, W. Zhu, S. Li, S. Li, J. Zheng, J. Chen, L. He, L. Jin, F. Pan, Y. Xiao, Twin boundary defect engineering improves lithium-ion diffusion for fast-charging spinel cathode materials, Nat. Commun. 12 (2021) 3085.

[27] S.C. Yin, Y.H. Rho, I. Swainson, L.F. Nazar, X-ray/neutron diffraction and electrochemical studies of lithium de/re-intercalation in $Li_{1-x}Co_{1/3}Ni_{1/3}Mn_{1/3}O_2$ ($x = 0 \rightarrow 1$), Chem. Mater. 18 (2006) 1901–1910.

[28] Q. Li, D. Ning, D. Zhou, K. An, D. Wong, L. Zhang, Z. Chen, G. Schuck, C. Schulz, Z. Xu, G. Schumacher, X. Liu, The effect of oxygen vacancy and spinel phase integration on both anionic and cationic redox in Li-rich cathode materials, J. Mater. Chem. A 8 (2020) 7733–7745.

[29] J.M. Clark, S. Nishimura, A. Yamada, M.S. Islam, High-voltage pyrophosphate cathode: Insights into local structure and lithium-diffusion pathways, Angew. Chem. Int. Ed. 51 (2012) 13149–13153.

[30] S. Nishimura, G. Kobayashi, K. Ohoyama, R. Kanno, M. Yashima, A. Yamada, Experimental visualization of lithium diffusion in Li_xFePO_4, Nat. Mater. 7 (2008) 707–711.

[31] C. Li, W.H. Kan, H. Xie, Y. Jiang, Z. Zhao, C. Zhu, Y. Xia, J. Zhang, K. Xu, D. Mu, F. Wu, Inducing favorable cation antisite by doping halogen in Ni-rich layered cathode with ultrahigh stability, Adv. Sci. 6 (2019) 1801406.

[32] E. Zhao, L. He, B. Wang, X. Li, J. Zhang, Y. Wu, J. Chen, S. Zhang, T. Liang, Y. Chen, X. Yu, H. Li, L. Chen, X. Huang, H. Chen, F. Wang, Structural and mechanistic revelations on high capacity cation-disordered Li-rich oxides for rechargeable Li-ion batteries, Energy Storage Mater. 16 (2019) 354–363.

[33] X.Y. Feng, C. Shen, X. Fang, C.H. Chen, Synthesis of $LiNi_{0.5}Mn_{1.5}O_4$ by solid-state reaction with improved electrochemical performance, J. Alloys Compd. 509 (2011) 3623–3626.

[34] M. Casas-Cabanas, C. Kim, J. Rodríguez-Carvajal, J. Cabana, Atomic defects during ordering transitions in $LiNi_{0.5}Mn_{1.5}O_4$ and their relationship with electrochemical properties, J. Mater. Chem. 4 (2016) 8255–8262.

[35] M. Reynaud, M. Casas-Cabanas, Order and disorder in NMC layered materials: A FAULTS simulation analysis, Powder Diffr. 32 (2017) S213–S220.

[36] E. Zhao, K. Wu, Z. Zhang, Z. Fu, H. Jiang, Y. Ke, W. Yin, K. Ikeda, T. Otomo, F. Wang, J. Zhao, Quantifying the anomalous local and nanostructure evolutions induced by lattice oxygen redox in lithium-rich cathodes, Small Methods 6 (2022) 2200740.

[37] E. Zhao, Q. Li, F. Meng, J. Liu, J. Wang, L. He, Z. Jiang, Q. Zhang, X. Yu, L. Gu, W. Yang, H. Li, F. Wang, X. Huang, Stabilizing the oxygen lattice and reversible oxygen redox chemistry through structural dimensionality in lithium-rich cathode oxides, Angew. Chem. Int. Ed. 58 (2019) 4323–4327.

[38] Q. Zhang, K. Liu, C. Li, S. Tan, L. Li, X.-G. Sun, W. Li, X. Liu, J. Zhang, S. Dai, The surface triple-coupling on single crystalline cathode for lithium ion batteries, Nano Energy 86 (2021) 106096.

[39] V.W.J. Verhoeven, F.M. Mulder, I.M. de Schepper, Influence of Mn by Li substitution on the Jahn–Teller distortion in $LiMn_2O_4$, Physica B 276–278 (2000) 950–951.

[40] A. Senyshyn, M.J. Muhlbauer, O. Dolotko, M. Hofmann, H. Ehrenberg, Homogeneity of lithium distribution in cylinder-type Li-ion batteries, Sci. Rep. 5 (2016) 18380.

[41] M.J. Mühlbauer, O. Dolotko, M. Hofmann, H. Ehrenberg, A. Senyshyn, Effect of fatigue/ageing on the lithium distribution in cylinder-type Li-ion batteries, J. Power Sources 348 (2017) 145–149.

[42] D. Petz, M.J. Mühlbauer, V. Baran, M. Frost, A. Schökel, C. Paulmann, Y. Chen, D. Garcés, A. Senyshyn, Lithium heterogeneities in cylinder-type Li-ion batteries—fatigue induced by cycling, J. Power Sources 448 (2020) 27466.

[43] D. Goonetilleke, J.C. Pramudita, M. Hagan, O.K. Al Bahri, W.K. Pang, V.K. Peterson, J. Groot, H. Berg, N. Sharma, Correlating cycling history with structural evolution in commercial 26650 batteries using in operando neutron powder diffraction, J. Power Sources 343 (2017) 446–457.

[44] W.K. Pang, V.K. Peterson, N. Sharma, J.-J. Shiu, S.-H. Wu, Lithium migration in $Li_4Ti_5O_{12}$ studied using in situ neutron powder diffraction, Chem. Mater. 26 (2014) 2318–2326.

[45] M. Catti, I. Pinus, K. Knight, Lithium insertion properties of $Li_xTiNb_2O_7$ investigated by neutron diffraction and first-principles modelling, J. Solid State Chem. 229 (2015) 19–25.

[46] K. Du, A. Gao, L. Gao, S. Sun, X. Lu, C. Yu, S. Li, H. Zhao, Y. Bai, Enhancing the structure stability of Ni-rich $LiNi_{0.6}Co_{0.2}Mn_{0.2}O_2$ cathode via encapsulating in negative thermal expansion nanocrystalline shell, Nano Energy 83 (2021) 105775.

[47] D. Goonetilleke, N. Sharma, W.K. Pang, V.K. Peterson, R. Petibon, J. Li, J.R. Dahn, Structural evolution and high-voltage structural stability of $Li(Ni_xMn_yCo_z)O_2$ electrodes, Chem. Mater. 31 (2018) 376–386.

[48] J. Liu, Z. Du, X. Wang, S. Tan, X. Wu, L. Geng, B. Song, P.-H. Chien, S.M. Everett, E. Hu, Anionic redox induced anomalous structural transition in Ni-rich cathodes, Energy Environ. Sci. 14 (2021) 6441–6454.

[49] C. Peabody, C.B. Arnold, The role of mechanically induced separator creep in lithium-ion battery capacity fade, J. Power Sources 196 (2011) 8147–8153.

[50] V.A. Sethuraman, N. Van Winkle, D.P. Abraham, A.F. Bower, P.R. Guduru, Real-time stress measurements in lithium-ion battery negative-electrodes, J. Power Sources 206 (2012) 334–342.

[51] X. Wu, B. Song, P.H. Chien, S.M. Everett, K. Zhao, J. Liu, Z. Du, Structural evolution and transition dynamics in lithium ion battery under fast charging: An operando neutron diffraction investigation, Adv. Sci. 8 (2021) 2102318.

[52] M.E. Ferraro, B.L. Trembacki, V.E. Brunini, D.R. Noble, S.A. Roberts, Electrode mesoscale as a collection of particles: Coupled electrochemical and mechanical analysis of NMC cathodes, J. Electrochem. Soc. 167 (2020) 013543.

[53] D.W. Dees, S. Kawauchi, D.P. Abraham, J. Prakash, Analysis of the galvanostatic intermittent titration technique (GITT) as applied to a lithium-ion porous electrode, J. Power Sources 189 (2009) 263–268.

[54] A. Nickol, T. Schied, C. Heubner, M. Schneider, A. Michaelis, M. Bobeth, G. Cuniberti, GITT analysis of lithium insertion cathodes for determining the lithium diffusion coefficient at low temperature: Challenges and pitfalls, J. Electrochem. Soc. 167 (2020) 090546.

[55] G. Hasegawa, N. Kuwata, Y. Tanaka, T. Miyazaki, N. Ishigaki, K. Takada, J. Kawamura, Tracer diffusion coefficients of Li^+ ions in *c*-axis oriented Li_xCoO_2 thin films measured by secondary ion mass spectrometry, Phys. Chem. Chem. Phys. 23 (2021) 2438–2448.

[56] Y. Wei, J. Zheng, S. Cui, X. Song, Y. Su, W. Deng, Z. Wu, X. Wang, W. Wang, M. Rao, Y. Lin, C. Wang, K. Amine, F. Pan, Kinetics tuning of Li-ion diffusion in layered $Li(Ni_xMn_yCo_z)O_2$, J. Am. Chem. Soc. 137 (2015) 8364–8367.

[57] C. Wang, R. Wang, Z. Huang, M. Chu, W. Ji, Z. Chen, T. Zhang, J. Zhai, H. Lu, S. Deng, J. Chen, L. He, T. Liang, F. Wang, J. Wang, Y. Deng, W. Cai, Y. Xiao, Unveiling the migration behavior of lithium ions in NCM/Graphite full cell via in operando neutron diffraction, Energy Storage Mater. 44 (2022) 1–9.

[58] H. Wang, Ning, L. Wang, H. Li, Q. Li, M. Ge, J. Zou, S. Chen, H. Shao, Y. Lai, Y. Zhang, G. Xing, W.K. Pang, Y. Tang, In Operando neutron scattering multiple-scale studies of lithium-ion batteries, Small 18 (2022) 2107491.

[59] L. Boulet-Roblin, D. Sheptyakov, P. Borel, C. Tessier, P. Novák, C. Villevieille, Crystal structure evolution *via* operando neutron diffraction during long-term cycling of a customized 5 V full Li-ion cylindrical cell $LiNi_{0.5}Mn_{1.5}O_4$ *vs.* graphite, J. Mater. Chem. 5 (2017) 25574–25582.

[60] M. Bianchini, E. Suard, L. Croguennec, C. Masquelier, Li-rich $Li_{1+x}Mn_{2-x}O_4$ spinel electrode materials: An operando neutron diffraction study during $Li^{\pm}$ extraction/insertion, J. Phys. Chem. C 118 (2014) 25947–25955.

[61] D. Liu, Z. Shadike, R. Lin, K. Qian, H. Li, K. Li, S. Wang, Q. Yu, M. Liu, S. Ganapathy, X. Qin, Q.-H. Yang, M. Wagemaker, F. Kang, X.-Q. Yang, B. Li, Review of recent development of in situ/operando characterization techniques for lithium battery research, Adv. Mater. 31 (2019) 1806620.

[62] D. Goonetilleke, T. Faulkner, V.K. Peterson, N. Sharma, Structural evidence for Mg-doped $LiFePO_4$ electrode polarisation in commercial Li-ion batteries, J. Power Sources 394 (2018) 1–8.

[63] Z. Huang, M. Chu, R. Wang, W. Zhu, W. Zhao, C. Wang, Y. Zhang, L. He, J. Chen, S. Deng, L. Mei, W.H. Kan, M. Avdeev, F. Pan, Y. Xiao, Optimizing the structure of layered cathode material for higher electrochemical performance by elucidating structural evolution during heat processing, Nano Energy 78 (2020) 105194.

[64] Y. Chen, K. An, Unraveling transition-metal-mediated stability of spinel oxide via in situ neutron scattering, J. Energy Chem. 68 (2022) 60–70.

[65] N. Sharma, V.K. Peterson, M.M. Elcombe, M. Avdeev, A.J. Studer, N. Blagojevic, R. Yusoff, N. Kamarulzaman, Structural changes in a commercial lithium-ion battery during electrochemical cycling: An in situ neutron diffraction study, J. Power Sources 195 (2010) 8258–8266.

[66] Q. Liu, S. Li, S.H. Wang, X.G. Zhang, S.S. Zhou, Y. Bai, J.Y. Zheng, X. Lu, Kinetically determined phase transition from stage II (LiC_{12}) to stage I (LiC_6) in a graphite anode for Li-ion batteries, J. Phys. Chem. Lett. 9 (2018) 5567–5573.

[67] X.Y. Song, K. Kinoshita, T.D. Tran, Microstructural characterization of lithiated graphite, J. Electrochem. Soc. 143 (1996) L120–L123.

[68] M. Drue, M. Seyring, M. Rettenmayr, Phase formation and microstructure in lithium-carbon intercalation compounds during lithium uptake and release, J. Power Sources 353 (2017) 58–66.

[69] D. Goonetilleke, N. Sharma, *In situ* neutron powder diffraction studies, Phys. Sci. Rev. 6 (2021) 20180155.

[70] S. Shiotani, T. Naka, M. Morishima, M. Yonemura, T. Kamiyama, Y. Ishikawa, Y. Ukyo, Y. Uchimoto, Z. Ogumi, Degradation analysis of 18650-type lithium-ion cells by *operando* neutron diffraction, J. Power Sources 325 (2016) 404–409.

[71] A. Senyshyn, M.J. Mühlbauer, O. Dolotko, H. Ehrenberg, Low-temperature performance of Li-ion batteries: The behavior of lithiated graphite, J. Power Sources 282 (2015) 235–240.

[72] B. Vadlamani, K. An, M. Jagannathan, K.S.R. Chandran, An in-situ electrochemical cell for neutron diffraction studies of phase transitions in small volume electrodes of Li-ion batteries, J. Electrochem. Soc. 161 (2014) A1731–A1741.

[73] I.A. Bobrikov, A.M. Balagurov, C.W. Hu, C.H. Lee, T.Y. Chen, S. Deleg, D.A. Balagurov, Structural evolution in $LiFePO_4$-based battery materials: *In-situ* and *ex-situ* time-of-flight neutron diffraction study, J. Power Sources 258 (2014) 356–364.

[74] H. Seo, B. Seong, K. Kim, C.W. Yi, Investigation of structural change and electrochemical reaction of spinel-$LiMn_2O_4$ by neutron diffraction, J. Ceram. Process. Res. 17 (2016) 472–477.

[75] U. Janakiraman, T.R. Garrick, M.E. Fortier, Review-lithium plating detection methods in Li-ion batteries, J. Electrochem. Soc. 167 (2020) 160552.

[76] B.V. Ratnakumar, M.C. Smart. Lithium Plating Behavior in Lithium-ion Cells, ECS Transactions, 2010.

[77] V. Zinth, C. von Luders, M. Hofmann, J. Hattendorff, I. Buchberger, S. Erhard, J. Rebelo-Kornmeier, A. Jossen, R. Gilles, Lithium plating in lithium-ion batteries at sub-ambient temperatures investigated by in situ neutron diffraction, J. Power Sources 271 (2014) 152–159.

[78] C. von Luders, V. Zinth, S.V. Erhard, P.J. Osswald, M. Hofmann, R. Gilles, A. Jossen, Lithium plating in lithium-ion batteries investigated by voltage relaxation and in situ neutron diffraction, J. Power Sources 342 (2017) 17–23.

[79] N. Legrand, B. Knosp, P. Desprez, F. Lapicque, S. Rael, Physical characterization of the charging process of a Li-ion battery and prediction of Li plating by electrochemical modelling, J. Power Sources 245 (2014) 208–216.

[80] L. Cai, K. An, Z.L. Feng, C.D. Liang, S.J. Harris, In-situ observation of inhomogeneous degradation in large format Li-ion cells by neutron diffraction, J. Power Sources 236 (2013) 163–168.

[81] L. Boulet-Roblin, D. Sheptyakov, P. Borel, C. Tessier, P. Novak, C. Villevieille, Crystal structure evolution via operando neutron diffraction during long-term cycling of a customized 5 V full Li-ion cylindrical cell $LiNi_{0.5}Mn_{1.5}O_4$ *vs.* graphite, J. Mater. Chem. A 5 (2017) 25574–25582.

[82] L. Cai, K. An, Z. Feng, C. Liang, S. Harris, J. In-situ observation of inhomogeneous degradation in large format Li-ion cells by neutron diffraction, J. Power Sources 236 (2013) 163–168.

[83] B. Song, I. Dhiman, J.C. Carothers, G.M. Veith, J. Liu, H.Z. Bilheux, A. Huq, Dynamic lithium distribution upon dendrite growth and shorting revealed by operando neutron imaging, ACS Energy Lett. 4 (2019) 2402–2408.

[84] C. Chen, J.F.M. Oudenhoven, D.L. Danilov, E. Vezhlev, L. Gao, N. Li, F.M. Mulder, R.-A. Eichel, P.H.L. Notten, Origin of degradation in Si-based all-solid-state Li-ion microbatteries, Adv. Energy Mater. 8 (2018) 1801430.

[85] F. Han, A.S. Westover, J. Yue, X. Fan, F. Wang, M. Chi, D.N. Leonard, N.J. Dudney, H. Wang, C. Wang, High electronic conductivity as the origin of lithium dendrite formation within solid electrolytes, Nat. Energy 4 (2019) 187–196.

Yuxi Luo received her B.S. degree in Zhiyuan College from Shanghai Jiao Tong University, P.R. China in 2022. She is pursuing her M.S. degree in Prof. Yinguo Xiao's group at School of Advanced Materials, Peking University, P.R. China. She focuses on layered cathode materials of lithium and sodium ion batteries through X-ray and neutron diffraction methods.

Xiaoyu Gao received her B.S. degree in School of Materials Science and Engineering from Tongji University, P.R. China in 2022. She is pursuing her M.S. degree in Prof. Yinguo Xiao's group at School of Advanced Materials, Peking University, P.R. China. She focuses on layered cathode materials of lithium ion batteries through X-ray and neutron diffraction methods.

Mingjie Dong received his B.S. degree in School of Mechanical, Electrical and Information Engineering from Shandong University, P.R. China in 2022. He is pursuing his M.S. degree in Prof. Yinguo Xiao's group at School of Advanced Materials, Peking University, P.R. China. He focuses on layered cathode materials of sodium ion batteries through X-ray and neutron diffraction methods.

Tao Zeng received his B.S. degree in School of Materials Science and Engineering from Xiangtan University, P.R. China in 2022. He is pursuing his M.S. degree in Prof. Yinguo Xiao's group at School of Advanced Materials, Peking University, P.R. China. He focuses on layered cathode materials of lithium ion batteries through X-ray and neutron diffraction methods.

Ziwei Chen received his bachelor's degree of engineering from the School of Material Science and Chemical engineering at Ningbo University in 2019. He is currently pursuing his Ph. D. degree in the School of Advanced Materials, Peking University under the supervision of Prof. Yinguo Xiao. His research interest is the synthesis of layered cathode materials and structure characterization based on X-ray and neutron diffraction methods.

Maolin Yang received his B.Eng. degree from the School of Chemistry and Chemical Engineering at Chongqing University in 2020. He is currently a Ph. D. candidate in the School of Advanced Materials, Peking University under the supervision of Prof. Yinguo Xiao. His research interests mainly focus on the synthesis of cathode materials for Li- and Na-ion batteries and their structural characterization based on X-ray and neutron diffraction methods.

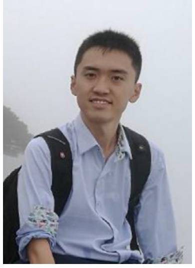

Zhongyuan Huang received his B.S. degree in Materials Science and Engineering from University of Science and Technology Beijing, P.R. China in 2018. He is pursuing his Ph. D. degree in Prof. Yinguo Xiao's group at School of Advanced Materials, Peking University, P.R. China. Currently, his research interest is electrode materials for LIBs and structural characterization based on X-ray and neutron diffraction techniques.

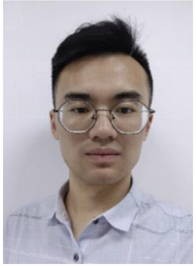

Rui Wang received his Ph. D. degree in the School of Advanced Materials, Peking University, China. His research interest is structural characterization for cathode materials of lithium ion battery using X-ray and neutron scattering technology.

Prof. Feng Pan, founding Dean of School of Advanced Materials, Peking University Shenzhen Graduate School, got B.S. from Dept. Chemistry, Peking University in 1985 and Ph.D. from Dept. of P&A Chemistry, University of Strathclyde, Glasgow, UK, with “Patrick D. Ritchie Prize” for the best Ph.D. in 1994. With more than a decade experience in large international incorporations, Prof. Pan has been engaged in fundamental research and product development of novel optoelectronic and energy storage materials and devices. As Chief Scientist, Prof. Pan led eight entities in Shenzhen to win 150 million RMB grant for the national new energy vehicles (power battery) innovation project since 2013.

Prof. Yinguo Xiao received his Ph.D. degree from Institute of Physics, Chinese Academy of Sciences, China in 2006. He was a postdoctoral fellow from 2007 to 2009 and a research scientist from 2009 to 2014 at Juelich Research Center (Forschungszentrum Jülich), Germany. He became a tenured staff scientist in Juelich Research Center since 2015. In 2017, he joined Peking University Shenzhen Graduate School, China as an associate professor. His research interests are on research and development of energy materials, magnetic materials, and characterization of complex materials using X-ray and neutron scattering techniques.